

# Black-Box Watermarking for Generative Adversarial Networks

Vladislav Skripniuk<sup>1</sup>, Ning Yu<sup>2,3</sup>, Sahar Abdelnabi<sup>1</sup>, and Mario Fritz<sup>1</sup>

<sup>1</sup>CISPA Helmholtz Center for Information Security

<sup>2</sup>Max Planck Institute for Informatics

<sup>3</sup>University of Maryland, College Park

## Abstract

As companies start using deep learning to provide value to their customers, the demand for solutions to protect the ownership of trained models becomes evident. Several watermarking approaches have been proposed for protecting discriminative models. However, rapid progress in the task of photorealistic image synthesis, boosted by Generative Adversarial Networks (GANs), raises an urgent need for extending protection to generative models.

We propose the first watermarking solution for GAN models. We leverage steganography techniques to watermark GAN training dataset, transfer the watermark from the dataset to GAN models, and then verify the watermark from generated images. In the experiments, we show that the hidden encoding characteristic of steganography allows preserving generation quality and supports the watermark secrecy against steganalysis attacks. We validate that our watermark verification is robust in wide ranges against several image perturbations. Critically, our solution treats GAN models as an independent component: watermark embedding is agnostic to GAN details and watermark verification relies only on accessing the APIs of black-box GANs.

We further extend our watermarking applications to generated image detection and attribution, which delivers a practical potential to facilitate forensics against deep fakes and responsibility tracking of GAN misuse.

## 1 Introduction

Deep Learning (DL) techniques, ranging from discriminative models [54, 46, 77, 81, 35] to generative models [45, 31, 69, 62, 44, 42, 9, 43], have achieved great success in many applications. They are now widely used and industrially deployed in part due to the availability of many open-source development infrastructures including Caffe [40], Theano [7], Torch [19], PyTorch [67], Chainer [84], and Tensorflow [1], that accelerated progress. Furthermore, academic and industrial researchers often publicize their state-of-the-art models'

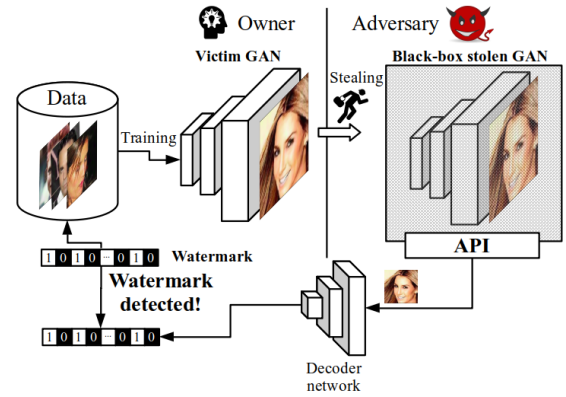


Figure 1: An overview of our black-box GAN watermarking solution.

implementations for function reproduction, which contributed to the dissemination of the latest results and advances.

As a result of this rapid progress and its availability, Machine Learning as a Service (MLaaS) has rapidly become a popular and profitable business (e.g., Amazon AWS ML [51], Microsoft Azure ML [53], Google Cloud AI [3], and IBM Watson ML [52]). However, training a commercial-level DL model is not a trivial task as it requires a large-scale dataset (e.g., ImageNet [22], CelebA [59], LSUN [92]), powerful computing resources (e.g., 8 NVIDIA Tesla V100 GPUs, \$8,000 each), in addition to significant DL expertise. It usually takes days up to weeks for training and requires an even longer time for many trial-and-error iterations on algorithm design, model architecture selection, and hyper-parameter search.

On the other hand, as DL models are difficult to train while easy to access, they become vulnerable to adversaries. Adversaries can redistribute an existing model with little effort and in turn provide a plagiarized DL service without citing or acknowledging the model owner. Such copyright infringement encroaches on the owner's credits and scoops the commercial potentials from the owner. In this sense, it becomes necessary and urgent to propose solutions for model Intellectual

Property (IP) protection, i.e., model ownership verification.

## 1.1 Model watermarking

As protecting models from copying, extraction, or stealing (even with limiting the access to black-box APIs) is challenging [65, 85], the commonly used defense against stealing models is model watermarking. This enables the identification of a stolen model and, thus, the verification of ownership, similar to IP legal protection of patents, trademarks, and copyright licenses [80, 48, 74].

The model watermarking procedure is composed of two phases: embedding and detection, and can be differentiated into two categories: black-box watermarking [2, 97] and white-box watermarking [86, 12, 21]. The embedding phase is to embed identification information into the model without affecting its utility. That identification information is called a watermark, which is provided by the owner and secret to others including potential adversaries.

In black-box watermarking, it is unnecessary to manipulate the model weights. Instead, the watermark is embedded as a special input-output behavior (similar to trigger sets in backdoor [32, 2]). A small set of inputs is selected and assigned with desirably unrelated outputs. Such special pairs are mixed with normal training pairs to train the model accordingly. The ownership of a watermarked model is detected based on the assumption that only with a very small probability a non-watermarked model can demonstrate the same behavior. In white-box watermarking, it is required to access the model weights. Then the watermark is explicitly embedded as part of the weight distributions using an invertible transformation. During detection, the weights are transformed back and compared to the watermark. Black-box watermarking has the advantage of not requiring the white-box access to the model weights which is a more realistic scenario as attackers are not likely to publicize the stolen models [97].

**GANs.** Unfortunately, the studies of aforementioned protection are limited to the discriminative models [54, 46, 77, 81, 35], e.g., classification tasks, where the models map from image domain to class probability domain. To the best of our knowledge, the protection for the other prominent DL models, the generative models [45, 31, 69, 62, 44, 42, 9, 43], is surprisingly lacking.

Generative models aim to synthesize photorealistic images, mapping from noise vector domain to image domain. In particular, Generative Adversarial Networks (GANs) techniques [31, 9, 43] have significantly pushed the edge of generated realism to a brand-new level, and have facilitated a variety of applications: image synthesis [31, 69, 33, 44, 9, 43], semantic image synthesis [66], super resolution [55], image attribute editing [15], text to image synthesis [96, 95], image to image translation [39, 103, 102], inpainting [93] and semi-supervised learning [78]. Open-source tool DeOldify [4] is a remarkable example of using GANs in image en-

hancement for colorizing and restoring old images and film footage.

**Three key challenges.** However, the development of watermarking solutions for GANs is lagged far behind their prevalence. It still urgently remains an open question of how to apply GAN watermarking. We identify three key challenges:

First, in discriminative models, there is a control over the input that would work as a trigger set for backdoor watermarking. In contrast, GANs require random sampling in the input domain which has to follow a natural prior distribution, e.g., a standard normal distribution. There is no control or pairing between noise vectors and generated images as this is learned in an unsupervised adversarial manner. Any specification on the pairs of noise and generated image gets biases from the natural prior distribution and impairs the entire generation fidelity, according to the practical disadvantage of VAE-GAN [49].

Second, in discriminative models, the outputs associated with the trigger set are assigned to a special target during supervised training. However, GANs are trained using only the unsupervised adversarial loss to approximate between two distributions which makes it difficult to assign a desirable special output for a trigger set. In addition, the image output domain of GANs is highly structured and full of semantics, making the output specification even more difficult to achieve.

Third, GAN training is known to be unstable due to its min-max formulation and alternation between gradient ascent/descent. Adding an auxiliary regularization term to the GAN objective could further amplify the training instability. Unlike watermarking for discriminative models [2, 98] where the original objective and the watermarking term are both reconstruction-based, any reconstructive auxiliary regularization cannot easily cooperate with the adversarial loss, according to the practical disadvantage of VAE-GAN [49].

These three challenges together imply to watermark a GAN without modifying the adversarial training. We, therefore, propose a black-box watermarking scheme. We sidestep from controlling the input-output behavior of GANs. In addition to its benefits in avoiding GAN training instability, a black-box solution better adheres to practical scenarios where we only have access to the stolen model APIs.

**GAN watermarking and deep fakes.** In addition to GAN model ownership verification, watermarking the output of GAN models is closely related to tracing the provenance of generated images (i.e., deep fakes) and attributing them to their respective GAN models [94, 89]. With the rapid ongoing progress [44, 42, 43], GANs learn to better match the target distribution which raises concerns about the future trajectories and misuse of powerful GANs [89, 23, 26, 6]. GAN watermarking can contribute to identifying watermarked generations from real images, and tracking responsibility in case of misuse (e.g., when the service is offered to different entities with different watermarks). Besides, models owners would

be motivated to cooperate with DL model administration platforms and watermark their models, in order to avoid liability for the potential misuse of their models. However, for this to be satisfied, the watermark should be verifiable from all or arbitrary outputs of the GAN model instead of a response to a specific trigger set (as typically used in discriminative model watermarking). Therefore, our GAN watermarking solution abandons the trigger set approach and aims to watermark all generated images.

## 1.2 Approach and contributions

To this end, we present the first black-box watermarking solution for GANs that we show in Figure 1. Unlike existing techniques that are only applicable to discriminative models, we propose to leverage steganography approaches [5, 83] to watermark the GAN training dataset, transfer the watermark from the dataset to the GAN model, and then verify the watermark from generated images. The model owner queries the APIs of a suspicious model and uses a pre-trained decoder to detect the watermark. If the detected watermark matches the owner’s watermark, it should form convincing legal evidence against the pirate. In addition, the watermark helps to identify generated images from real images and attribute them to their respective watermarked GANs.

**Image steganography meets GAN watermarking.** We differentiate between two important concepts: image steganography and model watermarking. Steganography aims to embed watermarks into images rather than networks, although sometimes the embedding and detection procedures are implemented by networks. Steganography is one way of protecting the IP of watermarked images, rather than models. We elaborate on the differences between these two concepts in Sections 2.1 and 2.3. We summarize the benefits of our approach of using image steganography (applied on the training dataset) to watermark GANs as follows:

1. It is a black-box watermarking solution that does not require access to GAN weights. It satisfies the practical scenario where the generation service usually publicizes only the APIs but not the model weights to users.
2. We leverage the secrecy and hidden encoding characteristics of steganography to guarantee the original generation performance.
3. It minimizes the possible incompatibility against GAN training by putting GAN in an independent component: it does not modify the original GAN training protocols, e.g., objective, network architecture, and optimization strategy. It acts as a plug-and-play watermarking pre-processing disentangled from GAN training and agnostic to GAN details.
4. As the watermark can be detected from all GAN generations (not a trigger set response), our solution offers

a way for tracing the responsibility of a watermarked GAN. This provides legal clues for malicious use cases of fake images. Our watermarking scheme increases the margin between real and fake images. It facilitates image forensics to separate real from fake images via extrinsic information (the watermark), considering real images are deterministically non-watermarked.

**Contributions.** Based on the above formulation, we summarize our contributions as follows:

1. To the best of our knowledge, this is the first study to formalize the problem of watermarking GAN models.
2. We empirically validate the effectiveness of our GAN watermarking solution. GANs learn the watermark from the dataset and deliver it to the generated images. As a result, it bridges the transferability between dataset watermarking and GAN model watermarking.
3. We further conduct comprehensive analysis to validate the fidelity, robustness, secrecy, and large capacity of our solution. In addition, we demonstrate the advantageous performance in two applications: generated image detection and image-to-GAN attribution.

## 2 Related work

In this section, we summarize the related work in the field including discriminative model watermarking, GANs, steganography, steganalysis, data poisoning, and GAN fingerprints.

### 2.1 Watermarking for discriminative models

We summarize previous watermarking works that focused on discriminative models. Based on the accessibility to model weights, they are typically categorized into white-box and black-box ones.

**White-box watermarking.** These methods require access to model weights or intermediate activations to perform ownership verification. Uchida et al. [86] proposed the first attempt to transform and embed watermarks into discriminative models weights via training regularization term, resulting in a white-box case. DeepMarks [12] and DeepSigns [21] have a similar flavor. They embed watermarks in the probability density function of model weights by leveraging the low probabilistic regions while minimizing the side effect to the classification accuracy and training overhead. White-box watermarking has limited use cases because the suspicious models are usually deployed remotely, and the plagiarized service would not publicize the parameters.

**Black-box watermarking.** In contrast, these methods do not require access to model weights and other details, e.g.,

architecture and training strategy. [2, 97, 50] embed watermarks in the input-output behavior of discriminative models; designing a specific trigger input set and associating it with specific class labels. Similarly, [57] focuses on making images in the trigger set visually indistinguishable from those in the regular set. Also, [82] embeds the watermark in predictions in order to defend against model extractions by APIs, by dynamically changing the responses for a small subset of queries. To address ambiguity attacks, [27] links the performance of a network with the presence of the correct watermark and substitutes the verification process with model fidelity evaluation.

However, previous protection studies are limited to discriminative models. To the best of our knowledge, the protection for the other prominent deep learning models, generative models, is surprisingly lacking. Our paper is the first to treat GANs as victim models and target IP protection of them.

## 2.2 Generative adversarial networks (GANs)

Photorealistic image generation can be viewed as the problem of sampling from the probability distribution of real-world images. To leverage the expressive power of deep learning, the sampling procedure is chosen to be a deep generative neural network with random noise as input. Training the generative model aims to approximate the generated distribution towards the real image distribution. This is challenging because the real image distribution is unknown and does not have a tractable distribution expression. GANs [31] introduce a workaround by formulating distribution approximation as a real/fake classification problem. GANs consist of two neural networks, a generator and a discriminator. The generator takes random noise as input and is trained to generate images as realistic as possible, while the discriminator receives images from both the generator and real dataset and is trained to differentiate the two sources. During training, these two networks compete and evolve simultaneously. GANs have significantly pushed the edge of generation realism to a brand-new level [69, 33, 44, 9, 43]. Successes in image domain have led to applications of GANs in many tasks, e.g., [66, 55, 15, 96, 95, 39, 93, 78].

However, the development of IP protection of GANs is lagged far behind the prevalence of GANs. It still urgently remains an open question how to apply watermarking protection to GANs, due to the three main challenges discussed in Section 1: the uncontrollable randomness of GANs input domain, the highly semantic structures of GANs output domain, and the unstable training. We propose to sidestep these challenges and present the first GAN watermarking solution.

## 2.3 Image steganography

We differentiate between two important concepts: image steganography and model watermarking (Section 2.1). Image

steganography represents a technique to hide information into carrier images in the initial purpose of covert communication [28]. It can also play a role in protecting the IP of carrier images if the hidden information is used as a watermark to verify the ownership of images [63, 88]. Although sometimes a steganography procedure is implemented by a network, it is never used nor directly able to hide information into a network and protect its IP.

Steganography has the advantage that the secret information is not obviously visible and its existence will not be suspected [60]. It avoids attracting the attention of adversaries and is subject to more control in an encrypted environment. Zero-bit steganography techniques [20, 10] modify the pixels of an image so that its Fourier transform lies in the cone with an owner defined direction. Least significant bit methods [68, 37, 38] hide information into images by minimizing the visual changes of image appearance. They distort information and fit it in the regions with more complex contexts, so as to make the traces less detectable. Several works proposed to substitute manually crafted hiding procedures with neural network embedding. [5, 34, 88, 99] use an encoder network to embed information in the latent space and use a decoder to detect that information from an image. [101] leverage data augmentation to improve the robustness of the two networks against perturbations such as blur, noise, crop, and JPEG compression. [83] presents a pipeline to detect hyperlinks from printed pictures. [98] releases an open-source implementation of a steganography system for hiding text messages inside high-resolution images. [76, 87] use GANs to generate cover images that improve the performance of steganography methods. [90] directly generates steganographic images without cover images.

We propose to leverage steganography approaches [5, 83] to watermark images in the GAN training dataset, then transfer the watermark from the dataset to the GAN model, and then detect the watermark from generated images. We take advantage of the secrecy characteristic of steganography to preserve the original generation performance. We separate the steganography procedure from GAN training to minimize the possible incompatibility between the two.

## 2.4 Image steganalysis

With the ever-growing advancements in steganography techniques, there has been equitable growth of research on steganalysis techniques as well, as a countermeasure for steganography. Image steganalysis techniques are proposed to prevent the transmission of secret information through images. Binary steganalysis typically solves the binary classification problem of whether or not there exists hidden information in an image. Spatial Rich Model [29] extracts spatial correlation information of high-frequency residuals of images and uses these features to train a binary classifier. [56] trains a classifier using an artificial training set, which is formed by



applying the targeted steganographic algorithm to the testing data. Then the classifier aims to differentiate between images on which the steganographic algorithm was applied once and those on which it was applied twice. [91] is the first to use neural networks for both feature extraction and binary classification. See [64, 41] for a comprehensive review of the development of binary steganalysis.

Though the binary steganalysis can help stall the illicit and unwanted communications, quantitative steganalysis endeavors to go beyond this identification and aims to dig out more information about the hidden message through various investigative steps and finally reconstruct the secret message [30]. Machine learning paradigms such as logistic regression [104], ensemble framework [18], extreme learning machines [17], and neural networks [13] have been used for quantitative steganalysis and hidden message regression. See [16] for a comprehensive review of quantitative steganalysis.

Image steganalysis techniques can also be used by adversaries to examine images and detect watermarks. We consider this as a possible attack in our threat model in Section 3.1 and employ [56] to test the secrecy of our GAN watermarking solution in Section 4.2.3.

## 2.5 Data poisoning

Several works study the use of training data to influence the behavior of discriminative models during test time. Data poisoning attacks [8, 79, 75] target to maliciously add a few data points to the training set, such that the trained model has to predict an unrelated label chosen by an adversary on particular samples. Backdoor attacks [14, 32] add into a class unrelated training samples with a trigger pattern; at test time, any sample with the same trigger will be classified in this class regardless of its semantics ground truth. In a similar spirit, [73] introduces imperceptible but “radioactive” perturbations into training data, such that any model trained on it will bear an identifiable mark. This is an effective example to show the transferability of identification information from training data to discriminative models. Inspired by its flavor but beyond that, we validate in this paper the transferability of image steganographic effect from training data to GANs, from a constructive perspective to protect the IP of generative models.

## 2.6 GAN fingerprints and deep fake detection

Images generated by GANs intrinsically bear unique fingerprints. [61] shows that GANs leave unique noise residuals to generated samples, which facilitate real/fake detection. [94] moves one step further, using a neural network classifier to attribute different images to their sources including a real-world source and various GAN sources. They show that it is even possible to finely differentiate samples from GANs which only differ in random seeds used for training. [89] also trains

a classifier and improves testing generalization ability across different generator domains. [100, 25, 24] show that GAN fingerprints are embedded in the high-frequency region of a spectrum, and [58] shows that fingerprints are recognizable from texture features.

Different from all these studies where attribution accuracy has to be contingent on the strengths and distinguishability of intrinsic fingerprints, we propose a watermarking solution that artificially embeds distinctive watermarks into GANs in an owner-controllable manner. It has an advantage that the margin between real and watermarked fake is amplified (Section 4.3), and ownership attribution is more accurately validated (Section 4.4).

## 3 Black-box GAN watermarking

We present the first black-box GAN watermarking approach that extends model watermarking beyond discriminative models. We first present our threat model and summarize five qualifications of a desirable watermarking solution in Section 3.1. Then we establish the watermarking pipeline in Section 3.2.

### 3.1 Threat model

In our analysis, we consider two threats: piracy and GAN misuse. In piracy, we consider a model owner and an adversary. The model owner invests resources into training a GAN model  $G$  and uses it to offer a generation service  $s$  to customers. The adversary pirates the well-trained  $G$  from the owner to obtain  $G'$ , and offers a similar service  $s'$ . Model piracy can be done via a malware attack or with the help of an insider. To detect piracy, in the white-box scenario verifying  $G \approx G'$  should be sufficient. But white-box is not a practical assumption because the adversary usually does not publicize the model weights. Therefore, in this paper, we consider the more practical black-box scenario where only  $s'$  (i.e., the output of  $G'$ ) is accessible to the owner. But verifying  $s \approx s'$  is not sufficient evidence of piracy because all generators ideally approximate their services towards the same real dataset distribution. In the second threat, the adversary uses generated images from a well-trained GAN (that could be offered by a black-box service) for malicious purposes, e.g., a possible flood of fake multimedia.

Therefore, in the black-box scenario and as shown in Figure 1, the owner seeks a watermarking solution by embedding a secret watermark  $w$  to  $G$  and obtains a watermarked model  $G_w$  that produces a generation service  $s_w$ . This helps the owner to prove ownership and, by cooperating with DL model administration platforms, to avoid the liability for potential misuse. Also, it helps to track the responsibility of misuse, if the service is distributed to different entities with different watermarks. Besides, it contributes to the visual forensics efforts by introducing an imperceptible, yet verifiable, watermark

in the generated images that facilitates its identification from real images. We formalize five qualifications for a desirable GAN watermarking system as follows:

1. **Effectiveness.** At the owner's end, an arbitrary watermark  $\mathbf{w}$  in a given form can be embedded into a GAN model  $G$  and should be accurately detected from  $s_{\mathbf{w}}$ , the generated images of a watermarked model  $G_{\mathbf{w}}$ . The detection should not depend on the access to the weights of  $G_{\mathbf{w}}$ , so as to abide by the black-box scenario in reality.
2. **Fidelity.** To preserve the utility of the service, a watermarked generator  $G_{\mathbf{w}}$  should provide a comparable service and generation quality to that of the original generator  $G$ , i.e.,  $s \approx s_{\mathbf{w}}$ . In addition, this avoids the adversary's suspect of the existence of a watermark, and therefore, avoids the counter-efforts that decrypt or remove the owner's watermark from the stolen service.
3. **Secrecy.** To avoid attacks that aim to remove the watermark and hinder its verification, the presence of the watermark  $\mathbf{w}$  should not be easily detected by the adversary. This requires the watermark to be secret enough under the adversary's steganalysis techniques.
4. **Robustness.** Regardless of the secrecy of the watermark, the adversary may always apply perturbation attacks to the generated images  $s'_{\mathbf{w}}$ . Therefore, at the owner end, the watermark should always be robustly detected from  $s'_{\mathbf{w}}$  given a possible range of perturbations (e.g., noise, blurring, JPEG compression, and cropping).
5. **Capacity.** The watermarking solution should have a large enough capacity to embed a large amount of information and maintain a large number of distinctive watermarks for different GAN models.

## 3.2 Watermarking pipeline

We model our watermarking solution such that it satisfies the previously mentioned qualifications. We demonstrate in Figure 2 the pipeline that consists of four stages, and describe it below in details.

### 3.2.1 Watermark encoder-decoder training

To embed the watermark into the GAN training dataset, we train an image steganography system on the owner side. The use of steganography techniques meets the **fidelity** and **secrecy** qualification of a desired watermarking system because it minimizes the effect on the generation quality and keeps the watermark hidden. The system is similar in spirit to [5, 83] and it consists of a jointly trained encoder-decoder architecture; the encoder is trained to imperceptibly embed an arbitrary watermark into arbitrary images, while the decoder

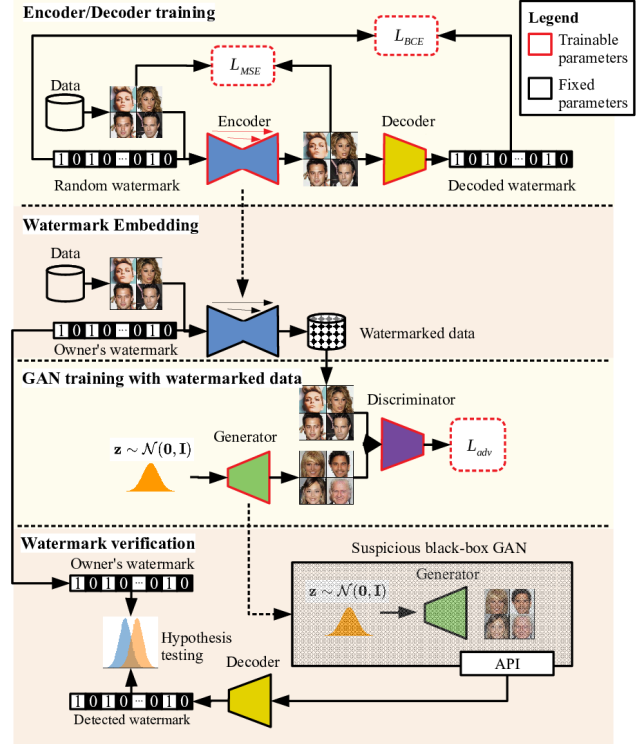


Figure 2: The four stages of our GAN watermarking pipeline. The first and third stages are in the training mode, while the second and fourth stages are in the inference mode.

is trained to detect that watermark. The watermark is represented as a sequence of  $n$  binary bits.  $n$  should be large enough to avoid a collision in a large space of all possible watermarks, meeting the **capacity** qualification.

The encoder  $E$  combines a cover image  $\mathbf{x}$  and a randomly sampled binary watermark  $\mathbf{w}$  as input, and maps them to a stego image  $\tilde{\mathbf{x}}$ :  $E(\mathbf{x}, \mathbf{w}) \mapsto \tilde{\mathbf{x}}$ . The stego image has the same size as that of the cover image and should be perceptually similar to it, i.e.,  $\mathbf{x} \approx \tilde{\mathbf{x}}$ . The decoder  $D$  takes the stego image  $\tilde{\mathbf{x}}$  as input and aims to reconstruct watermark:  $D(\tilde{\mathbf{x}}) \mapsto \tilde{\mathbf{w}}$  and desirably  $\tilde{\mathbf{w}} \approx \mathbf{w}$ . We achieve the above by jointly training the encoder and decoder w.r.t. the following objective:

$$\min_{E,D} \mathbb{E}_{\mathbf{x} \sim \text{real}, \mathbf{w} \sim \{0,1\}^n} L_{BCE}(\mathbf{x}, \mathbf{w}; E, D) + \lambda L_{MSE}(\mathbf{x}, \mathbf{w}; E) \quad (1)$$

$$L_{BCE}(\mathbf{x}, \mathbf{w}; E, D) = \frac{1}{n} \sum_{k=1}^n (\mathbf{w}_k \log \tilde{\mathbf{w}}_k + (1 - \mathbf{w}_k) \log(1 - \tilde{\mathbf{w}}_k)) \quad (2)$$

$$L_{MSE}(\mathbf{x}, \mathbf{w}; E) = \|E(\mathbf{x}, \mathbf{w}) - \mathbf{x}\|_2^2 \quad (3)$$

$$\tilde{\mathbf{w}} = D(E(\mathbf{x}, \mathbf{w})) \quad (4)$$

where  $\mathbf{w}_k$  and  $\tilde{\mathbf{w}}_k$  are the  $k$ th bits of the watermarks  $\mathbf{w}$  and  $\tilde{\mathbf{w}}$  separately; and  $\lambda$  is a hyper-parameter to balance the two objective terms. The binary cross-entropy term  $L_{BCE}$  guides the decoder to decode whatever binary watermark sequence that is embedded by the encoder. The mean squared error term  $L_{MSE}$  penalizes any deviation of the stego image  $\tilde{\mathbf{x}}$  from the original cover image  $\mathbf{x}$ .

### 3.2.2 Watermark embedding to GAN training dataset

The second stage is the inference mode of the first stage after the training of encoder and decoder converges. The owner defines a watermark and uses the encoder to embed it into each real image of the GAN training dataset. By this stage, the watermark appears in the carrier of images.

### 3.2.3 GAN training with the watermarked dataset

Our watermarking solution is motivated by not introducing instability to the GAN training, for the purpose of preserving the utility. Therefore, it is independent of GAN training, agnostic to all its details, and acts as a plug-and-play pre-processing. In the third stage, the owner trains a GAN model in the original manner using the watermarked dataset. We assume by this stage that the watermark can be effectively transferred from training images to the generations of the GAN model. If this holds, the owner can trustingly publicize the model which has been imperceptibly watermarked. We call it a watermarked GAN. We empirically validate it meets the **effectiveness** qualification in Section 4.2.1.

### 3.2.4 Watermark verification

The fourth stage is the inference mode of the third stage. The owner performs the watermark verification to either prove ownership to a suspicious GAN model or track the responsibility of distributed models in case of misuse. To be qualified in practice, we model for the black-box scenario where the owner does not require access to the GAN weights. The owner only needs to have a generated image  $\mathbf{x}'$  (the misused image or a one obtained by the APIs queries), and detects its watermark  $\mathbf{w}' = D(\mathbf{x}')$  using the well-trained decoder from the first stage. Then the owner compares the detected watermark  $\mathbf{w}'$  to the original watermark  $\mathbf{w}$ , and observes  $k$  matching bits. Instead of exact matching, we verify the watermark by hypothesis testing given the number of matching bits (where the null hypothesis is getting these matching bits by chance). As we validate in Section 4.2.4, this is sufficient for the detection of the watermark even after applying perturbations to the generated images. As a result, it meets the **robustness** qualification.

In specific, we consider two hypotheses:

$H_0 : \mathbf{w}' \neq \mathbf{w}$ , some bits are matching due to random coincidence;

$$H_1 : \mathbf{w}' \approx \mathbf{w}$$

Under the null hypothesis  $H_0$ , the probability of the number of matching bits, denoted as the random variable  $K$ , follows a binomial distribution with  $n = \dim(\mathbf{w})$  trials and 0.5 probability of success. Given the observation of  $k$  matching bits, the owner computes the p-value, the probability of the extreme cases where there are  $k$  or even more matching bits under  $H_0$ .

$$p = Pr(K \geq k | H_0) = \sum_{i=k}^n \binom{n}{i} 0.5^n \quad (5)$$

The watermark verification holds if and only if the p-value is smaller than a small threshold  $\tau$ , which corresponds to the situation where  $k$  is larger than a large threshold  $\kappa$ . In another word, if the owner observes a large number of matching bits, it is very unlikely to accept the null hypothesis  $H_0$ , meaning to instead accept  $H_1$  that  $\mathbf{w}'$  and  $\mathbf{w}$  match. In Section 4.2.1 we do not explicitly set  $\tau$ . Rather, we derive how to set up a reasonable threshold  $\kappa$  and validate, by this stage, the transferability of the presence of watermark from training dataset to GAN model, which can then be verified by the generated images.

## 4 Experiments

The goal of this section is to validate the five qualifications of our black-box watermarking solution (Sections 4.2.2-4.2.5). Sections 4.3 and 4.4 show that watermarking is beneficial to solve two tasks related to digital forensics: detection and attribution of generated images.

### 4.1 Implementation details

**Encoder.** The encoder is trained to embed a watermark into a cover image while minimizing the perceptual differences between the input and stego images. We follow the technical details proposed in [83]. The watermark binary vector is first passed through a fully-connected layer and then reshaped as a tensor with one channel dimension and with the same spatial dimension of the cover image. We then concatenate this watermark tensor and the image along the channel dimension as the input to a U-Net [72] style architecture. The output of the encoder, the stego image, has the same size as that of the cover image. Note that passing the watermark through a fully-connected layer allows for every bit of the binary sequence to be encoded over the entire spatial dimensions of the cover image and flexible to the coverage image size. In our experiments, the image size is set to  $128 \times 128 \times 3$  without losing representativeness. The watermark length is set to 100 as suggested in [83]. The length of 100 binary bits leads to a large enough space for watermark design as well as does not deteriorate the original performance perceptually. We visualize the encoder architecture in Figure 3.

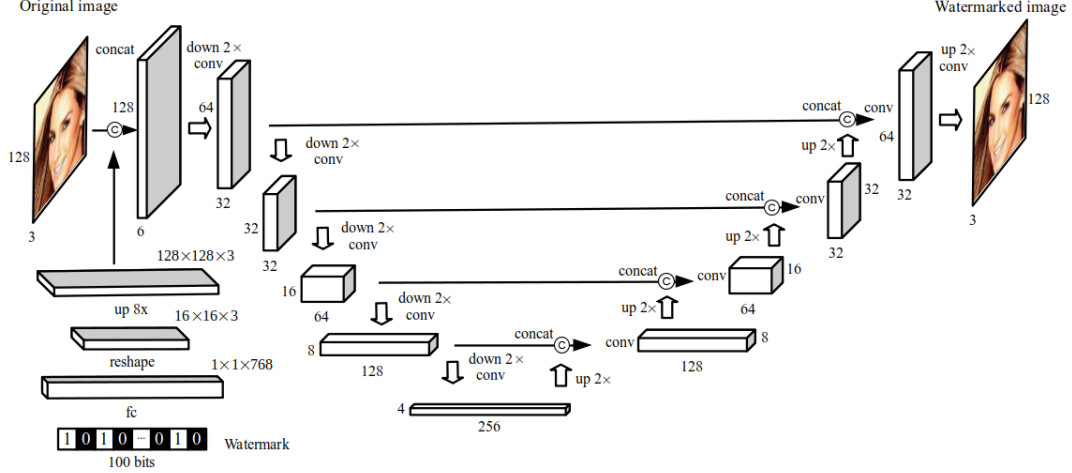


Figure 3: Encoder architecture.

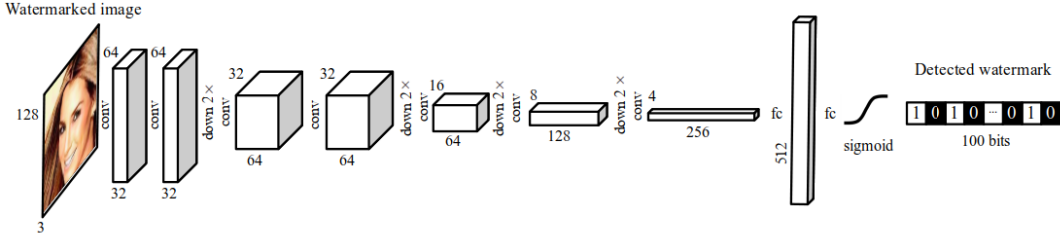


Figure 4: Decoder architecture.

**Decoder.** The decoder is trained to recover the hidden watermark from the stego image. We follow the technical details proposed in [83]. It consists of a series of convolutional layers with kernel size  $3 \times 3$  and strides  $\geq 1$ , dense layers, and a sigmoid output activation to produce a final output with the same length as the watermark binary vector. We visualize the encoder architecture in Figure 4.

**Encoder and decoder training.** The encoder and decoder are jointly trained end-to-end w.r.t. the objective in Eq. 1. We randomly sample watermark binary vectors and embed them to the images from either MNIST digit dataset [54] (60,000 training images and 10,000 testing images), CelebA face dataset [59] (150,000 train images and 50,000 testing images) or LSUN bedroom dataset [92] (50,000 training images and 50,000 testing images). The encoder is trained to balance watermark reconstruction and image reconstruction. At the beginning of training, we set  $\lambda = 0$  to focus on watermark reconstruction, otherwise watermarks cannot be accurately embedded into cover images. After the watermark detection accuracy achieves 95% (that takes 3-5 epochs), we increase  $\lambda$  linearly up to 10 within 3,000 iterations to shift our focus more on cover image reconstruction. We train the encoder and decoder for 30 epochs in total. Given the batch size of 64, it takes 3 hours using 1 NVIDIA Tesla V100 GPU with

16GB memory.

**Victim GAN models.** One of the advantages of our watermarking solution is to disentangle watermarking from GAN training and put GAN details in an independent component. Therefore, without losing representativeness, we selected two milestone works of GAN techniques, DCGAN [69] and ProGAN [44], as the victim GAN models for watermark embedding and detection. Model training is implemented in PyTorch in a way agnostic to watermarking and equivalent to official implementations on GitHub [70, 71]. In order to obtain corresponding watermarked GAN, model training is run with our watermarked MNIST digit dataset, watermarked CelebA face dataset, or watermarked LSUN bedroom dataset.

## 4.2 Qualifications of our GAN watermarking

In this section, we design comprehensive experiments to evaluate our GAN watermarking solution w.r.t. the five desirable qualifications formalized in Section 3.1: effectiveness, fidelity, security, robustness, and capacity. We discuss different evaluation metrics, compared baseline methods, and/or analysis studies for each qualification, if applicable, to validate the advantages and/or working ranges of our solution.



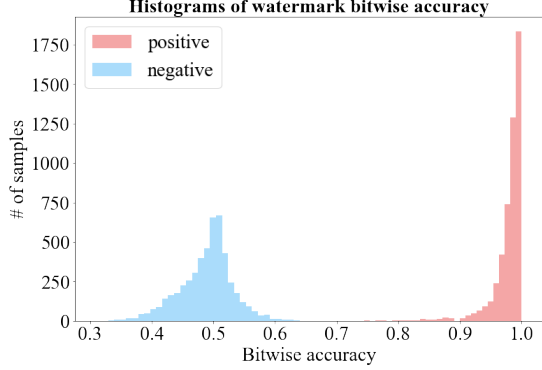


Figure 5: Histograms of watermark bitwise accuracy given positive (red) or negative samples (blue). They are evaluated on ProGAN on CelebA. The positive samples are generated by the owner’s watermarked GAN model. The negative samples are either from the real world, or generated by a non-watermarked GAN model or by another watermarked GAN model different from the owner’s. We can perceive a significant margin to distinguish the two distributions, which validates the 99.67% precision of our solution.

#### 4.2.1 Effectiveness

At the owner’s end, the effectiveness of the watermark verification, i.e., the capability of embedding arbitrary watermarks into a GAN model and detecting them in a black-box scenario (only from generated images), is the key qualification. If we validate this, we can also empirically redeem our assumptions in Sec 3.2 into important discoveries: the transferability of the presence of watermark from training images to GAN model and then to generated images.

**Evaluations.** In our experiments, the effectiveness is successively evaluated by two types of performance: *precision* and *recall*. The definitions in this paper are different from those in the traditional classification tasks. Here precision measures the classification accuracy of whether or not a testing image is generated by the owner’s watermarked GAN, while recall measures the watermark detection accuracy given a testing image from the owner’s watermarked GAN. Both precision and recall are calculated based on the *bitwise accuracy* between the owner’s watermark ground truth  $\mathbf{w}$  and the detected watermark  $\mathbf{w}'$ . We elaborate on each below.

**Precision.** The classification was conducted by thresholding on the bitwise accuracy. Given ProGAN on CelebA, we looped over 10,000 testing images. Half of the testing images are positive samples, i.e., generated by the owner’s watermarked GAN model, and the other half of the images are negative samples, i.e., either from the real world (counting for 1/6 of the testing images), or generated by a non-watermarked GAN model (counting for 1/6 of the testing images) or by another watermarked GAN model different from the owner’s (counting for 1/6 of the testing images).

In principle, the bitwise accuracy for the negative samples

should resemble that of random guess, the histogram of which should follow the binomial distribution with parameters  $n = 100$  (the length of watermark) and  $p = 0.5$  (unbiased binary random guess). In contrast, the bitwise accuracy for the positive samples should have a much higher value in statistics, leading to a distinguishable histogram distribution from that of the negative samples.

We plot and compare the two histograms in Figure 5. They are visually distinguishable with a significant margin. In terms of quantitative evaluation, we set the classification threshold as 0.75, which is around the middle point of the margin. It means the owner’s watermarked GAN model is verified if the number of matching bits is more than 75% of the watermark length. It also derives to set  $\kappa = 0.75n = 75$  for Section 3.2.4, which corresponds to a reasonable significance level  $\tau < 10^{-6}$  according to Eq. 5. Compared to the ground truth, it results in 99.67% precision. Consequently, the precision of our watermarking solution is validated and we can move on to more comprehensive comparisons w.r.t. recall given all the testing images generated by the owner’s watermarked GAN models.

**Recall.** We report in the third and fourth columns of Table 1 two metrics to evaluate recall, both the higher the better. In the watermark bit level, we calculate the mean bitwise accuracy over 10,000 testing images generated by the owner’s watermarked GAN model. In the instance level, we count the instance detection accuracy, i.e. the percentage of those images where the owner’s watermarks are detected. We keep setting  $\kappa = 75$  according to the precision calculation. In the second column of Table 1 we calculate as a reference the mean bitwise accuracy where the images are the watermarked GAN training images. In the fifth column, we report as a reference the p-value (Eq. 5) to accept  $H_0$ .

**Baseline.** For comparisons, since there is no existing work on GAN watermarking, we designed a straightforward baseline method for an alternative consideration. Instead of watermarking GAN training data, we enforce watermark reconstruction jointly with GAN training. In another words, we enforce each generated image to not only look realistic approximating the real training data, but also contain the owner’s watermark. Mathematically,

$$\min_{G,D} \max_{Dis} \mathbb{E}_{\mathbf{z} \sim \mathcal{N}(\mathbf{0}, \mathbf{I}), \mathbf{x} \sim \text{real}} L_{adv}(\mathbf{z}, \mathbf{x}; G, Dis) + \eta \mathbb{E}_{\mathbf{z} \sim \mathcal{N}(\mathbf{0}, \mathbf{I}), \mathbf{w} \sim \{0,1\}^n} L_{BCE}(\mathbf{z}, \mathbf{w}; G, D) \quad (6)$$

where  $G$  and  $Dis$  are the original generator and discriminator in GAN framework,  $L_{adv}$  is the original GAN objective, and  $L_{BCE}$  is adapted from Eq. 2 where we replace  $\tilde{\mathbf{w}} = D(E(\mathbf{x}, \mathbf{w}))$  with  $\tilde{\mathbf{w}} = D(G(\mathbf{z}))$ .  $\eta$  is a hyper-parameter to balance the two objective terms. By tuning  $\eta$  we obtained two extremes of results: either  $L_{adv}$  or  $L_{BCE}$  dominates training. When  $L_{adv}$  dominates, the generated images have high visual quality but watermark detection is close to random guess. When  $L_{BCE}$  dominates, watermarks are accurately

Model & Dataset	Train bit acc	Gen bit acc	Instance acc	p-value accept $H_0$
DCGAN MNIST (bsl)	1.00	0.49	0.00	0.61
DCGAN MNIST	1.00	0.97	1.00	$< 10^{-24}$
ProGAN MNIST	1.00	0.96	1.00	$< 10^{-23}$
ProGAN CelebA	1.00	0.98	1.00	$< 10^{-26}$
ProGAN LSUN	1.00	0.93	1.00	$< 10^{-19}$

Table 1: Two recall evaluations: watermark bitwise accuracy of testing images generated by the owner’s watermarked GAN (third column) and instance detection accuracy of those images (fourth column). As references, the second column shows the bitwise accuracy of images that are watermarked GAN training images; the fifth column shows the p-value to accept the null hypothesis  $H_0$  in Section 3.2.4. The “bsl” row corresponds to the baseline method subject to Eq. 6 where we merge watermark reconstruction into GAN training.

detected but the generation quality deteriorates heavily. We finally report in Table 1 with  $\eta = 1.0$  where we tended to guarantee the generation quality.

**Results.** From Table 1 we summarize:

(1) The watermarking baseline (the “bsl” row) method completely fails with bitwise accuracy of 0.49, close to binary random guess, and instance detection accuracy 0.0, equal to blind rejection. The failure indicates GAN watermarking is a challenging task. Directly combining a watermarking objective with GAN training is easily incompatible. In contrast, our solution of leveraging image steganography and transferring watermarking from GAN training datasets to GAN models sidesteps the possible incompatibility and leads to advantageous performance. See below.

(2) According to the instance accuracy, our watermarking solution results in perfect detection (100% accuracy) with negligible p-values to accept the null hypothesis  $H_0$ . It validates our effective watermark recall with a significant margin, agnostic to GAN models and datasets.

(3) According to the bitwise accuracy, our watermarking solution results in almost saturated accuracy ( $\geq 93\%$  accuracy), i.e., no obvious deterioration from that of the watermarked training data. It indicates the learning of our watermark generation is effective, with information drops by  $\leq 7\%$ .

(4) Refer to the differences of watermark bitwise accuracy, we notice a GAN model can foster more accurate watermark detection ( $\geq 96\%$ ) if the original generation task is easier (MNIST and CelebA against LSUN). We interpret that the task of learning the watermark becomes entangled with the task of learning the distribution of real images. The more effective a GAN model learns the dataset distribution, the more effective watermarks can be transferred from the training dataset to the model.

(5) Combining the success in precision and recall measurements, we validate the effectiveness of our watermark

Dataset	Source	FID (non-watermarked)	FID (watermarked)
CelebA	Data	0.60	1.76
CelebA	ProGAN	14.09	14.38
LSUN	Data	0.61	4.16
LSUN	ProGAN	50.74	50.42

Table 2: FID comparisons between samples with or without watermark.

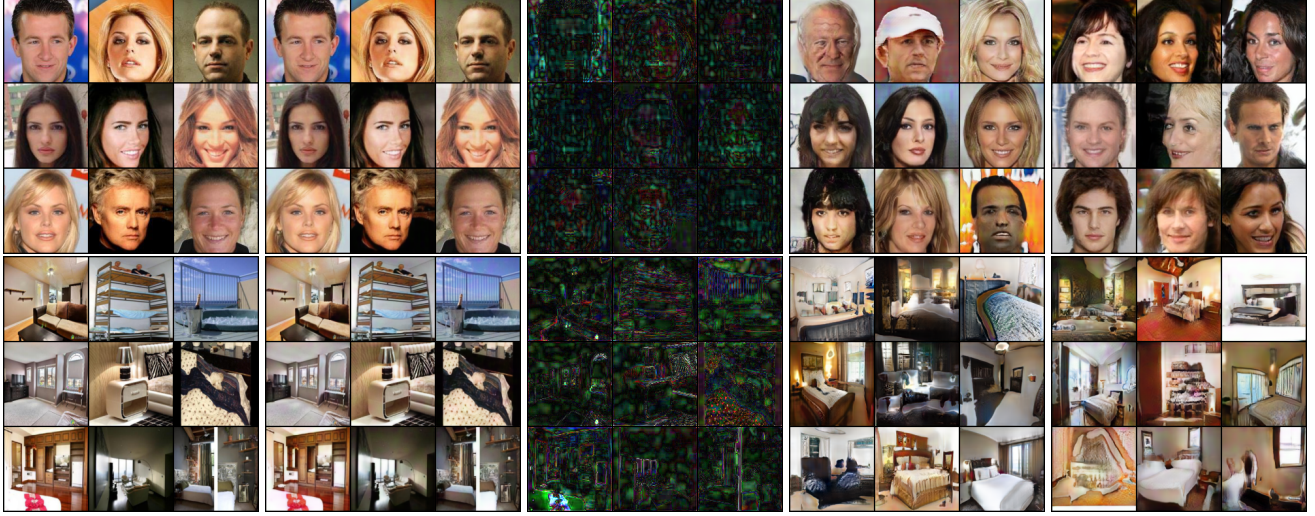
solution, and validate the transferability of the presence of watermark from training images to GAN model and then to generated images.

## 4.2.2 Fidelity

The fidelity of a watermarked GAN is as critical as the watermarking effectiveness. It requires a watermarked GAN to preserve its original generation quality. On one hand, the owner preserves the utility of the service. On the other hand, it avoids the adversary’s suspect of the existence of the watermark. In principle, the steganography technique we used should enable this, and we validate it below.

**Evaluation.** In GAN studies, generation quality is commonly evaluated by Fréchet Inception Distance (FID) [36], which is the major pursuit of most GAN models. It first embeds a real reference dataset and a generation set respectively through a fixed ImageNet-pretrained Inception network [81], and then measures the Kullback–Leibler divergence [47] of the two embedding sets as the distance, the smaller the higher generation quality. We also use FID to evaluate generation quality and compare between 50,000 images generated by a watermarked GAN and another 50,000 images generated by a non-watermarked GAN, in order to validate the fidelity of the former. To calculate FID in different settings, the real reference dataset is kept unchanged.

**Results.** We show in Table 2 the FID comparisons of ProGAN on CelebA or LSUN. As a reference, we report in the first and third rows the FID of GAN training data, with or without being watermarked. We find: In the second and fourth rows, compared to the non-watermarked models, our watermarked models preserve generation quality with the FID fluctuating within a range of  $\pm 2.1\%$ , although, in the first and third rows, the FID of training data fluctuates much heavily ( $\pm 582\%$ ). It validates, although watermarking deteriorates GAN training data, it does not affect the generation fidelity in practice. This is because the generated results are not as realistic as the real data, and therefore not as sensitive to watermarking as the real data. In practice, the generated watermarks are naturally hidden by the original GAN artifacts. See Figure 6 for demonstrations.



(a) Original GAN training samples. (b) Watermarked GAN training samples. (c) Difference between 6a and 6b (10× magnified). (d) Samples from the non-watermarked GAN. (e) Samples from the watermarked GAN.

Figure 6: Qualitative comparisons for Table 2. (Top row - CelebA, bottom row - LSUN.)

Attack	Watermark detection acc
White-box encoder (strong)	0.946
Unknown encoder (weak)	0.502

Table 3: Watermark detection accuracy of ATS attacks.

### 4.2.3 Secrecy

The presence of a watermark embedded in a GAN model should not be easily detected by the adversary, otherwise, it would be potentially removed by the adversary and confuse the watermark verification. This qualification is more demanding than fidelity, because high fidelity avoids the adversary’s visual detection while secrecy requires technical counter-detection against steganalysis.

**Attacks and evaluation.** In order to design a quantitative evaluation on secrecy, we consider from the adversary side a binary classification problem: the presence of watermark in an image. We propose to make the attack stronger by equipping the adversary with more knowledge and allow attacks to the earliest stage of our watermarking pipeline. Namely, we assume the adversary is aware of our steganographic technique in Section 3.2.1 and proposes to classify if an image sampled from the real world is watermarked or not. This assumption favors the adversary side. If the adversary fails to detect the watermark in GAN training data, it is even more difficult to detect it from the later stages, because GAN training will potentially make the presence of watermark more ambiguous to some extent, according to the drop of watermark bitwise accuracy in Table 1.

On the adversary side, we follow the attack protocol in [101] to perform the Artificial Training Sets (ATS) experi-

ment [56]. We target to separate testing images watermarked 0 or 1 time without supervision. The attack is as follows. We suppose we have another encoder on the adversary side corresponding to the victim steganographic technique. On one hand, we regard the original testing images as negative training samples. On the other hand, we apply the encoder twice to the testing set to obtain images watermarked 2 or 3 times, which are regarded as positive training samples. Then we train an SVM classifier [11] using such positive and negative samples, in order to separate images watermarked 0-1 time or 2-3 times. During testing, we first apply the encoder once to the testing images so that their ground truths are being watermarked 1 or 2 times. Then we can use our SVM to separate them and propagates the predictions back to the original images.

We consider a strong adversary and a weak adversary, which are contingent on their knowledge of the victim steganographic technique. The strong adversary somehow has white-box access to the owner’s encoder (is aware of the encoder weights) and is aware of the watermark that was used to generate watermarked images. Therefore, the adversary can use the owner’s encoder directly to launch the attack. The weak adversary is only aware of the architecture and training details of the owner’s encoder, and therefore, has to train a shadow encoder from scratch. In our experiments, the shadow encoder training is the same as in Section 3.2.1, just different in initialization.

We evaluate the adversary’s performance on a set of 250 watermarked real images and 250 non-watermarked real images.

**Results.** We report the strong and weak adversaries’ classification accuracy on CelebA in table 3. We find:



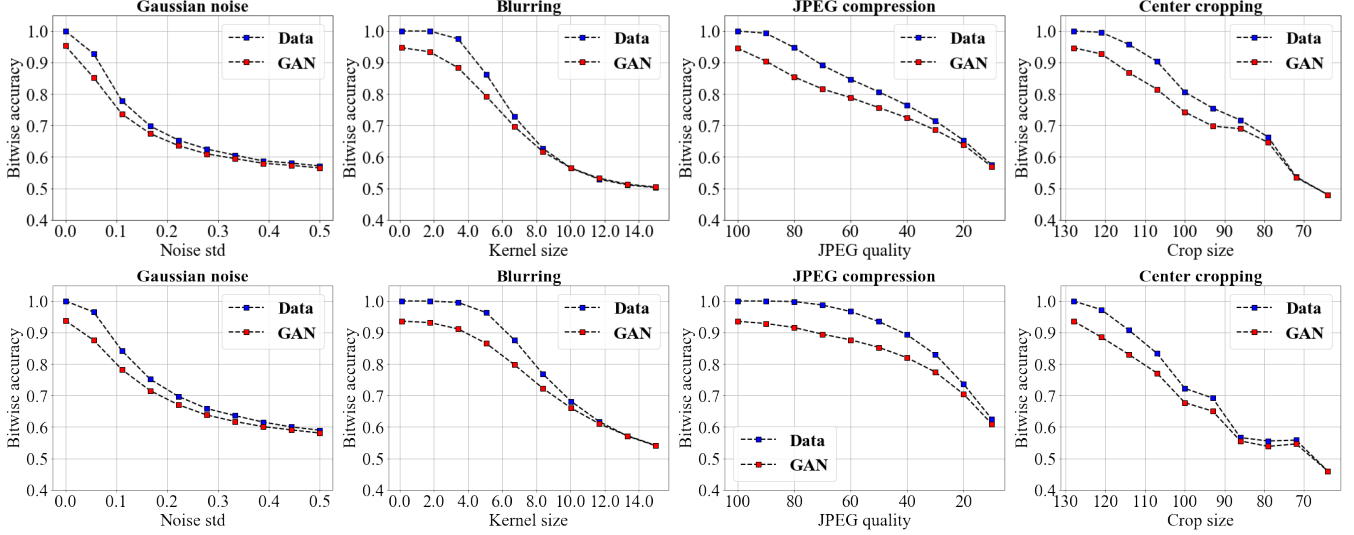


Figure 7: Watermark bitwise accuracy w.r.t. the amount of perturbations. Red dots represent detection on the watermarked GAN generated samples. Blue dots represent detection on the watermarked GAN training samples, which serve as the upper bound references for the red dots. (Top row - CelebA, bottom row - LSUN.)

(1) The strong adversary (the first row) achieves watermark detection with almost perfect accuracy (94.6%) ascribed to the access to the targeted encoder. It reminds the owner to not publicize the well-trained encoder after using our watermarking solution. This is a feasible suggestion because publicizing the GAN model alone is sufficient to provide the generation service.

(2) The weak adversary (the second row), in contrast, fails to detect the watermark with just random guess performance ( $\sim 50\%$  accuracy) because of lacking access to the targeted encoder weights. That indicates encoders trained from different initialization use different patterns to hide the watermark. In conclusion, if the owner keeps the weights of the original encoder private, the presence of watermark in the publicized GAN model is validated secret from the ATS attack.

#### 4.2.4 Robustness

The adversary may always apply perturbation attacks to the generated images regardless of the evidence of the watermark. Therefore, at the owner’s end, the watermark should always be robustly detected from a possible range of perturbations.

**Perturbation attacks and evaluation.** In this section we evaluate the robustness of our watermarking solution against four types of image perturbations: additive Gaussian noise, blurring with Gaussian kernel, JPEG compression, and center cropping. We vary the magnitude of each perturbation, apply it to the generated images from a watermarked GAN model, and use the well-trained decoder to detect watermark from the perturbed images. We evaluate w.r.t. the mean watermark bitwise accuracy over 10,000 perturbed images from watermarked ProGAN on either CelebA or LSUN, as we do for effectiveness evaluation in Section 4.2.1.

Original	Gaussian noise	Blurring	JPEG compression	Center cropping
99 bits	77 bits	75 bits	75 bits	80 bits
94 bits	80 bits	83 bits	84 bits	80 bits

Table 4: The number of detected bits (out of 100) from watermarked GAN samples. The detection performs robustly even when the image quality (utility) heavily deteriorates w.r.t. each perturbation.

**Results.** We plot in red dots in Figure 7 and the bitwise accuracy w.r.t. the magnitude of perturbations. As a reference for upper bound, we also plot the bitwise accuracy in blue dots if we apply varying perturbations to the watermarked GAN training images. Recall in Table 1 the first column, non-perturbed watermarked training images result in saturated detection accuracy. We summarize:

(1) For all the perturbations, watermark bitwise accuracy drops monotonously as we increase the magnitude of perturbation, while for small perturbations accuracy drops rather slowly. We consider accepting accuracy  $\geq 75\%$  according to the classification threshold in the above precision calculation. Consequently, we list the general working range w.r.t. each perturbation: Gaussian noise standard deviation  $\sim [0.0, 0.05]$ , Gaussian blur kernel size  $\sim [0, 5]$ , JPEG compression quality  $\sim [50, 100]$ , and center cropping size  $\sim [86, 128]$ , which are pretty wide ranges in practice.

(2) For the perturbations out of the above working ranges,



the reference upper bounds drop even faster and the margins to the testing curves shrink quickly, indicating the detection deterioration is not factually dominated by GAN training, but rather by the heavy image quality deterioration.

(3) As a result of (2), the adversary has to deteriorate an image with strong perturbations in order to suppress the watermark detection not better than random guess ( $\sim 50\%$  accuracy). However, that also destroys the utility of the service if the adversary tends to escape from being detected, making the adversary’s efforts invalid.

(4) As complementary to (3), we demonstrate in Table 4 how each perturbation affects the sample appearance, and how severely the image quality (utility) deteriorates w.r.t. each perturbation before the detection turns ineffective.

(5) As a conclusion, our watermarking solution is robust against four types of perturbations. It leads to wide working ranges in practice and guarantees that the stolen or misused service is detected until its utility is heavily perturbed.

#### 4.2.5 Capacity

A watermarking solution should have a large enough capacity to embed a large amount of information and maintain a large number of distinctive watermarks for different GAN models. In our experiments the capacity correlates to the length of the watermark, i.e., the number of bits  $n$  in the watermark. On one hand, a larger  $n$  leads to a larger watermark space and more likely avoids collision. On the other hand, however, a larger  $n$  may deteriorate the quality of watermarked images, according to the empirical analysis in [83]. Given the image size of  $128 \times 128 \times 3$ , it is recommended to use  $n = 100$ , as we have set for the other experiments.

**Evaluation.** In this section, we propose to explore the capacity boundary of our watermark space. It is just unnecessary to investigate a too large  $n$  considering the fidelity. The analysis is irrelevant to our watermarking pipeline, but rather the empirical relation between the maximal number of non-collided watermarks  $N$  w.r.t. the watermark length  $n$ . We define the concept of *collision* as: when two sampled watermarks have a number of matching bits that is higher than the verification threshold ( $\geq 75\%$  as per the setting in Section 4.2.1).

Given each  $n$ , we simulate the watermark sampling process. We sample watermarks one by one, and check if a watermark collides against any existing watermark in the database. If so, we stop the simulation and report the database size as the maximal value of  $N$ ; if not, we add the current watermark to the database and sample the next watermark. We repeat this simulation 100 times for each  $n$  and report the average for robustness consideration.

**Result.** For  $n = 100$ , we empirically obtain  $N = 2,355$  in average before the first collision happens. It means our solution can unambiguously operate 2,355 unique watermarks at the same time. For  $n = 200, 300, 500$ , and  $1,000$ , we are able

Method	Seen GAN model	Unseen GAN model
Classifier	0.997	0.508
Watermark	1.0	1.0

Table 5: Real/Fake classification accuracy. The first column corresponds to the scenario where the GAN model used for training covers that used for testing. The second column is the opposite scenario which is a more generalized situation.

to increase the database size up to 100,000 without collision.

### 4.3 Generated image detection

The breakthrough of GANs narrows the gap in visual quality between generated and real images. That makes the detection of generated images an increasing challenge. Recent concerns about deep fakes [26] and misuse of GANs raise demands for reliable detection methods. In this section, based on the validated qualifications of our watermarking solution, we extend it to an application that facilitates detecting samples from a watermarked GAN, for the purpose of increasing the margin between real and fake while at no cost of generation fidelity.

The problem of generated image detection is typically formulated as a binary classification problem: separating real from fake images. Unlike existing methods that detect intrinsic differences between the two classes [94, 100, 24], we propose to enhance the classification performance by embedding an artificial watermark into generated images, in contrast to real images which are deterministically non-watermarked. In particular, we regulate GAN owners to publicize only watermarked GAN models using our solution. Then we convert the problem to classifying if one image is watermarked or not. We use the same detection criterion as in Section 4.2.1, i.e., checking if the detected watermark of a testing image contains  $\geq 75\%$  matching bits to our reference watermark.

**Baseline.** We compare to a plain convolutional neural network (CNN) classifier as a baseline method, as implemented in [94]. It is trained on 10,000 CelebA real images and 10,000 images from a watermarked ProGAN. We consider two scenarios depending on whether or not the GAN model used for classifier training covers that used for testing.

**Results.** We report in Table 5 the classification accuracy over 1,000 CelebA real images and 1,000 images generated by a watermarked ProGAN. We find:

(1) Real/Fake classification based on watermark performs equally perfect ( $\sim 100\%$  accuracy) to that based on CNN classifier in the seen GAN scenario.

(2) More advantageously, our watermark-based classifier performs equally well over unseen GAN models while CNN classifier deteriorates to random guess ( $\sim 50\%$  accuracy). This is because CNN classifier is troubled by the domain gap between training and testing GAN models. In contrast,

our method enjoys the advantage of being agnostic to GAN models as it depends only on the presence of watermark rather than intrinsic information that is overfitting to a closed world discriminative task.

(3) This proposes a useful practice for DL model administration platforms to regulate model publication: publicizing a watermarked GAN model significantly decreases its deep fake risks in case of being misused.

#### 4.4 Image-to-GAN attribution

The goal of the image-to-GAN attribution task is to figure out the GAN model that generated a particular fake image. It plays an important role in tracing the responsibility of a GAN model, which provides legal clues for malicious use cases of fake images. Our watermarking solution, for the purpose of ownership verification, is qualified in principal for attribution. This is validated by the transferability of the watermark from GAN models to generated images.

**Closed world scenario.** In the closed world scenario, the model space is finite and known in advance. In our experiment, we train four ProGAN models on CelebA using four different watermarks. The task is to classify a mixture of 1,000 images evenly generated by these four models. To attribute images using watermarks, we apply our decoder to detect the watermark in the image, and assign that image to the GAN with the closest watermark.

**Open world scenario.** We further consider the open world scenario to validate if an attribution approach can accurately reject images from unknown GANs. In our experiment, the set of GANs is extended to two more watermarked ProGAN on CelebA, the watermarks of which are unknown. Along with the original task in the closed world, the new task also requires to classify 500 additional images evenly generated by these two GANs, meaning to label them as not belonging to any of the four known GANs. Our watermarking approach classifies an image as unknown if and only if the number of matching bits between the detected watermark and the closest known watermark is less than  $\kappa = 75$  out of 100.

**Baseline.** Yu et al. [94] use a plain CNN classifier to solve image-to-GAN attribution as a multi-class classification problem, which is limited to a closed world. We followed their protocol in the closed world scenario: training over 20,000 images generated evenly by each of the four GANs. We also extend their method to the open world scenario via training four one-vs-all-the-others binary classifiers. To train the  $i$ -th classifier we balance our sampling by using 10,000 images from the  $i$ -th GAN and another 10,000 images evenly from all the other GANs. During testing, all the four classifiers are applied to an image. We assign to the image the class with the highest confidence if not all the classifiers reject that image. Otherwise, we assign the image to the unknown label.

**Results.** We report in Table 6 the testing attribution accuracy. We find similar results to those in Section 4.3:

Method	Closed world	Open world
Classifier	0.998	0.235
Watermark	1.000	1.000

Table 6: Image attribution accuracy.

(1) Image attribution based on watermark performs equally perfect ( $\sim 100\%$  accuracy) to that based on CNN classifier in the closed world.

(2) More advantageously, our watermarking approach performs equally well in the open world scenario while CNN classifier deteriorates severely. This is because the four classifiers generalize poorly to the unknown GANs such that they attribute less than a quarter of unknown images correctly as unknown. In contrast, our method enjoys the advantage of being agnostic to GAN models as it depends only on the presence of watermark rather than intrinsic information that is overfitting to a closed world discriminative task.

(3) This proposes a useful practice for DL model administration platforms to regulate model publication: publicizing a watermarked GAN model significantly facilitates image attribution and responsibility tracking in case the generated images are misused.

## 5 Conclusion

In this paper, we propose the first black-box watermarking solution for protecting the Intelligent Property of generative adversarial networks. We first analyze the threat model in the black-box scenario, and formalize five qualifications for desired watermarking. In our pipeline, we leverage steganography techniques to watermark GAN training dataset, transfer the watermark from the dataset to GAN models, and then verify the watermark from generated images. In the experiments, we validate the effectiveness (watermark transferability), fidelity (no deterioration on generation quality), secrecy (against steganalysis), robustness (against image perturbations), and large capacity of our solution. Notably, the advantageous performance treats GAN models as an independent component: watermark embedding is agnostic to GAN details and watermark verification relies only on accessing the APIs of black-box GANs. We further extend our watermarking applications to generated image detection and attribution, which delivers a practical potential to facilitate forensics against deep fakes and responsibility tracking of GAN misuse.

## 6 Acknowledgement

We thank Matthew Tancik for sharing code and Apratim Bhat-tacharyya for constructive discussion and advice.

## References

- [1] Mart n Abadi et al. “Tensorflow: Large-scale machine learning on heterogeneous distributed systems”. In: *arXiv*. 2016.
- [2] Yossi Adi et al. “Turning your weakness into a strength: Watermarking deep neural networks by backdooring”. In: *USENIX Security*. 2018.
- [3] Google Cloud AI. In: URL: <https://cloud.google.com/products/ai>.
- [4] Jason Antic. *DeOldify. A Deep Learning based project for colorizing and restoring old images (and video!)* URL: [https://github.com/Newmu/dcgan\\_code](https://github.com/Newmu/dcgan_code).
- [5] Shumeet Baluja. “Hiding images in plain sight: Deep steganography”. In: *NeurIPS*. 2017.
- [6] In the age of a.i. is seeing still believing? In: URL: <https://www.newyorker.com/magazine/2018/11/12/in-the-age-of-ai-is-seeing-still-believing>.
- [7] James Bergstra et al. “Theano: a CPU and GPU math expression compiler”. In: *Proceedings of the Python for scientific computing conference (SciPy)*. 2010.
- [8] Battista Biggio, Blaine Nelson, and Pavel Laskov. “Poisoning attacks against support vector machines”. In: *ICML*. 2012.
- [9] Andrew Brock, Jeff Donahue, and Karen Simonyan. “Large scale gan training for high fidelity natural image synthesis”. In: *ICLR*. 2019.
- [10] Francois Cayre, Caroline Fontaine, and Teddy Furon. “Watermarking security: theory and practice”. In: *IEEE Transactions on signal processing*. 2005.
- [11] Chih-Chung Chang and Chih-Jen Lin. “LIBSVM: A library for support vector machines”. In: *ACM transactions on intelligent systems and technology*. 2011.
- [12] Huili Chen, Bit a Darvish Rohani, and Farinaz Koushanfar. “Deepmarks: A digital fingerprinting framework for deep neural networks”. In: *ICMR*. 2019.
- [13] Mo Chen, Mehdi Boroumand, and Jessica Fridrich. “Deep learning regressors for quantitative steganalysis”. In: *SPIE Electronic Imaging*. 2018.
- [14] Xinyun Chen et al. “Targeted backdoor attacks on deep learning systems using data poisoning”. In: *arXiv*. 2017.
- [15] Yunjey Choi et al. “Stargan: Unified generative adversarial networks for multi-domain image-to-image translation”. In: *CVPR*. 2018.
- [16] Shaveta Chutani and Anjali Goyal. “A review of forensic approaches to digital image Steganalysis”. In: *Multimedia Tools and Applications*. 2019.
- [17] Shaveta Chutani and Anjali Goyal. “Improved universal quantitative steganalysis in spatial domain using ELM ensemble”. In: *Multimedia Tools and Applications*. 2018.
- [18] Remi Cogranne and Jessica Fridrich. “Modeling and extending the ensemble classifier for steganalysis of digital images using hypothesis testing theory”. In: *IEEE Transactions on Information Forensics and Security*. 2015.
- [19] Ronan Collobert, Koray Kavukcuoglu, and Clément Farabet. “Torch7: A matlab-like environment for machine learning”. In: *NuerIPS workshop*. 2011.
- [20] Ingemar Cox et al. *Digital watermarking*. Springer, 2002.
- [21] Bit a Darvish Rouhani, Huili Chen, and Farinaz Koushanfar. “Deepsigns: An end-to-end watermarking framework for ownership protection of deep neural networks”. In: *ASPLOS*. 2019.
- [22] Jia Deng et al. “Imagenet: A large-scale hierarchical image database”. In: *CVPR*. 2009.
- [23] You thought fake news was bad? deep fakes are where truth goes to die. In: URL: <https://www.theguardian.com/technology/2018/nov/12/deep-fakes-fake-news-truth>.
- [24] Ricard Durall, Margret Keuper, and Janis Keuper. “Watch your Up-Convolution: CNN Based Generative Deep Neural Networks are failing to reproduce Spectral Distributions”. In: *CVPR*. 2020.
- [25] Ricard Durall et al. “Unmasking DeepFakes with simple Features”. In: *arXiv*. 2019.
- [26] Deep fakes. In: URL: <https://www.nbcnews.com/mach/video/deep-fakes-how-they-are-made-and-how-they-can-be-detected-1354417219989>.
- [27] Lixin Fan, Kam Woh Ng, and Chee Seng Chan. “Rethinking deep neural network ownership verification: Embedding passports to defeat ambiguity attacks”. In: *NeurIPS*. 2019.
- [28] Jessica Fridrich. *Steganography in digital media: principles, algorithms, and applications*. Cambridge University Press, 2009.
- [29] Jessica Fridrich and Jan Kodovsky. “Rich models for steganalysis of digital images”. In: *IEEE Transactions on Information Forensics and Security*. 2012.

- [30] Jessica Fridrich et al. “Forensic steganalysis: determining the stego key in spatial domain steganography”. In: *SPIE Security, Steganography, and Watermarking of Multimedia Contents*. 2005.
- [31] Ian Goodfellow et al. “Generative adversarial nets”. In: *NeurIPS*. 2014.
- [32] Tianyu Gu et al. “Badnets: Evaluating backdooring attacks on deep neural networks”. In: *IEEE Access*. 2019.
- [33] Ishaan Gulrajani et al. “Improved training of wasserstein gans”. In: *NeurIPS*. 2017.
- [34] Jamie Hayes and George Danezis. “Generating steganographic images via adversarial training”. In: *NeurIPS*. 2017.
- [35] Kaiming He et al. “Deep residual learning for image recognition”. In: *CVPR*. 2016.
- [36] Martin Heusel et al. “Gans trained by a two time-scale update rule converge to a local nash equilibrium”. In: *NeurIPS*. 2017.
- [37] Vojtěch Holub and Jessica Fridrich. “Designing steganographic distortion using directional filters”. In: *International Workshop on Information Forensics and Security*. 2012.
- [38] Vojtěch Holub, Jessica Fridrich, and Tomáš Dene-mark. “Universal distortion function for steganography in an arbitrary domain”. In: *EURASIP Journal on Information Security*. 2014.
- [39] Phillip Isola et al. “Image-to-image translation with conditional adversarial networks”. In: *CVPR*. 2017.
- [40] Yangqing Jia et al. “Caffe: Convolutional architecture for fast feature embedding”. In: *MM*. 2014.
- [41] Konstantinos Karampidis, Ergina Kavallieratou, and Giorgos Papadourakis. “A review of image steganalysis techniques for digital forensics”. In: *Journal of information security and applications*. 2018.
- [42] Tero Karras, Samuli Laine, and Timo Aila. “A style-based generator architecture for generative adversarial networks”. In: *CVPR*. 2019.
- [43] Tero Karras et al. “Analyzing and Improving the Image Quality of StyleGAN”. In: *CVPR*. 2020.
- [44] Tero Karras et al. “Progressive Growing of GANs for Improved Quality, Stability, and Variation”. In: *ICLR*. 2018.
- [45] Diederik P Kingma and Max Welling. “Auto-encoding variational bayes”. In: *ICLR*. 2014.
- [46] Alex Krizhevsky, Ilya Sutskever, and Geoffrey E Hinton. “Imagenet classification with deep convolutional neural networks”. In: *NeurIPS*. 2012.
- [47] S Kullback and RA Leibler. “On Information and Sufficiency”. In: *Annals of Mathematical Statistics*. 1951.
- [48] Gerhard C Langelaar, Iwan Setyawan, and Reginald L Lagendijk. “Watermarking digital image and video data. A state-of-the-art overview”. In: *IEEE Signal processing magazine*. 2000.
- [49] Anders Boesen Lindbo Larsen et al. “Autoencoding beyond pixels using a learned similarity metric”. In: *ICML*. 2016.
- [50] Erwan Le Merrer, Patrick Perez, and Gilles Trédan. “Adversarial frontier stitching for remote neural network watermarking”. In: *Neural Computing and Applications*. 2019.
- [51] Amazon AWS Machine Learning. In: URL: <https://aws.amazon.com/machine-learning>.
- [52] IBM Watson Machine Learning. In: URL: <https://www.ibm.com/cloud/machine-learning>.
- [53] Microsoft Azure Machine Learning. In: URL: <https://azure.microsoft.com/en-us/services/machine-learning>.
- [54] Yann LeCun et al. “Gradient-based learning applied to document recognition”. In: *Proceedings of the IEEE*. 1998.
- [55] Christian Ledig et al. “Photo-realistic single image super-resolution using a generative adversarial network”. In: *CVPR*. 2017.
- [56] Daniel Lerch-Hostalot and David Megias. “Unsupervised steganalysis based on artificial training sets”. In: *Engineering Applications of Artificial Intelligence*. 2016.
- [57] Zheng Li et al. “How to Prove Your Model Belongs to You: A Blind-Watermark based Framework to Protect Intellectual Property of DNN”. In: *ACSAC*. 2019.
- [58] Zhengzhe Liu et al. “Global Texture Enhancement for Fake Face Detection in the Wild”. In: *CoRR*. 2020.
- [59] Ziwei Liu et al. “Deep Learning Face Attributes in the Wild”. In: *ICCV*. 2015.
- [60] Xiaorong Lu et al. “A Secure and Robust Covert Channel Based on Secret Sharing Scheme”. In: *Asia-Pacific Web Conference*. 2016.
- [61] Francesco Marra et al. “Do gans leave artificial fingerprints?” In: *MIPR*. 2019.
- [62] Takeru Miyato et al. “Spectral normalization for generative adversarial networks”. In: *ICLR*. 2018.
- [63] Seung-Min Mun et al. “A robust blind watermarking using convolutional neural network”. In: *arXiv*. 2017.



- [64] Arooj Nissar and Ajaz Hussain Mir. “Classification of steganalysis techniques: A study”. In: *Digital Signal Processing*. 2010.
- [65] Tribhuvanesh Orekondy, Bernt Schiele, and Mario Fritz. “Knockoff nets: Stealing functionality of black-box models”. In: *CVPR*. 2019.
- [66] Taesung Park et al. “Semantic image synthesis with spatially-adaptive normalization”. In: *CVPR*. 2019.
- [67] Adam Paszke et al. “PyTorch”. In: 2016. URL: <https://github.com/pytorch/pytorch>.
- [68] Tomáš Pevn, Tomáš Filler, and Patrick Bas. “Using high-dimensional image models to perform highly undetectable steganography”. In: *International Workshop on Information Hiding*. 2010.
- [69] Alec Radford, Luke Metz, and Soumith Chintala. “Unsupervised representation learning with deep convolutional generative adversarial networks”. In: *ICLR*. 2016.
- [70] DCGAN GitHub Repository. In: URL: [https://github.com/Newmu/dcgan\\_code](https://github.com/Newmu/dcgan_code).
- [71] ProGAN GitHub Repository. In: URL: [https://github.com/tkarras/progressive\\_growing\\_of\\_gans](https://github.com/tkarras/progressive_growing_of_gans).
- [72] Olaf Ronneberger, Philipp Fischer, and Thomas Brox. “U-net: Convolutional networks for biomedical image segmentation”. In: *MICCAI*. 2015.
- [73] Alexandre Sablayrolles et al. “Radioactive data: tracing through training”. In: *arXiv*. 2020.
- [74] Lalit Kumar Saini and Vishal Shrivastava. “A survey of digital watermarking techniques and its applications”. In: *IJCST*. 2014.
- [75] Ali Shafahi et al. “Poison frogs! targeted clean-label poisoning attacks on neural networks”. In: *NeurIPS*. 2018.
- [76] Haichao Shi et al. “SSGAN: secure steganography based on generative adversarial networks”. In: *Pacific Rim Conference on Multimedia*. 2017.
- [77] Karen Simonyan and Andrew Zisserman. “Very deep convolutional networks for large-scale image recognition”. In: *ICLR*. 2015.
- [78] Jost Tobias Springenberg. “Unsupervised and semi-supervised learning with categorical generative adversarial networks”. In: *ICLR*. 2016.
- [79] Jacob Steinhardt, Pang Wei W Koh, and Percy S Liang. “Certified defenses for data poisoning attacks”. In: *NeurIPS*. 2017.
- [80] Mitchell D Swanson, Mei Kobayashi, and Ahmed H Tewfik. “Multimedia data-embedding and watermarking technologies”. In: *Proceedings of the IEEE*. 1998.
- [81] Christian Szegedy et al. “Going deeper with convolutions”. In: *CVPR*. 2015.
- [82] Sebastian Szyller et al. “Dawn: Dynamic adversarial watermarking of neural networks”. In: *arXiv*. 2019.
- [83] Matthew Tancik, Ben Mildenhall, and Ren Ng. “Stegastamp: Invisible hyperlinks in physical photographs”. In: *CVPR*. 2020.
- [84] Seiya Tokui et al. “Chainer: a next-generation open source framework for deep learning”. In: *NeurIPS workshop*. 2015.
- [85] Florian Tramèr et al. “Stealing machine learning models via prediction apis”. In: *USENIX Security*. 2016.
- [86] Yusuke Uchida et al. “Embedding watermarks into deep neural networks”. In: *ICMR*. 2017.
- [87] Denis Volkhonskiy, Ivan Nazarov, and Evgeny Burnaev. “Steganographic generative adversarial networks”. In: *ICMV*. 2020.
- [88] Vedran Vukotić, Vivien Chappelier, and Teddy Furon. “Are Deep Neural Networks good for blind image watermarking?” In: *International Workshop on Information Forensics and Security*. 2018.
- [89] Sheng-Yu Wang et al. “CNN-generated images are surprisingly easy to spot... for now”. In: *CVPR*. 2020.
- [90] Zihan Wang et al. “SSStGAN: self-learning steganography based on generative adversarial networks”. In: *ICONIP*. 2018.
- [91] Jian Ye, Jiangqun Ni, and Yang Yi. “Deep learning hierarchical representations for image steganalysis”. In: *IEEE Transactions on Information Forensics and Security*. 2017.
- [92] Fisher Yu et al. “Lsun: Construction of a large-scale image dataset using deep learning with humans in the loop”. In: *arXiv*. 2015.
- [93] Jiahui Yu et al. “Generative image inpainting with contextual attention”. In: *CVPR*. 2018.
- [94] Ning Yu, Larry S Davis, and Mario Fritz. “Attributing fake images to gans: Learning and analyzing gan fingerprints”. In: *ICCV*. 2019.
- [95] Han Zhang et al. “Stackgan++: Realistic image synthesis with stacked generative adversarial networks”. In: *TPAMI*. 2018.
- [96] Han Zhang et al. “Stackgan: Text to photo-realistic image synthesis with stacked generative adversarial networks”. In: *ICCV*. 2017.
- [97] Jialong Zhang et al. “Protecting intellectual property of deep neural networks with watermarking”. In: *Asia CCS*. 2018.

- [98] Kevin Alex Zhang et al. “SteganoGAN: high capacity image steganography with gans”. In: *arXiv*. 2019.
- [99] Ru Zhang, Shiqi Dong, and Jianyi Liu. “Invisible steganography via generative adversarial networks”. In: *Multimedia Tools and Applications*. 2019.
- [100] Xu Zhang, Svebor Karaman, and Shih-Fu Chang. “Detecting and simulating artifacts in gan fake images”. In: *International Workshop on Information Forensics and Security*. 2019.
- [101] Jiren Zhu et al. “Hidden: Hiding data with deep networks”. In: *ECCV*. 2018.
- [102] Jun-Yan Zhu et al. “Toward multimodal image-to-image translation”. In: *NeurIPS*. 2017.
- [103] Jun-Yan Zhu et al. “Unpaired image-to-image translation using cycle-consistent adversarial networks”. In: *ICCV*. 2017.
- [104] Djemel Ziou and Reza Jafari. “Efficient steganalysis of images: learning is good for anticipation”. In: *Pattern Analysis and Applications*. 2014.